

Intermediates in extrachromosomal homologous recombination in *Xenopus laevis* oocytes: characterization by electron microscopy

Geneviève Pont-Kingdon, Renée J. Dawson and Dana Carroll

Department of Biochemistry, University of Utah School of Medicine, Salt Lake City, UT 84132, USA

Communicated by B. Dujon

Several molecular mechanisms have been proposed to account for nonconservative homologous recombination. This type of recombination is particularly efficient in *Xenopus* oocytes when appropriate DNA substrates are injected. To distinguish between possible models, we have investigated recombination intermediates from oocytes by direct observation in the electron microscope. Partially recombined DNA was crosslinked with a psoralen derivative after incubation in oocytes to limit the branch migration that might occur during recovery procedures and alter the structures that were initially present. Branched structures, which we interpret as intermediates, represented ~10% of the DNA recovered and were readily analyzed. We did not observe any structures with internal loops predicted by invasion mechanisms. The majority of intermediates had one or two single-stranded branches on product-sized molecules, as predicted for incomplete junctions in the resection–annealing mechanism. Detailed length measurements confirmed the expectations of that model. When recovered DNA was not crosslinked, or when annealed junctions were prepared *in vitro*, we saw branched structures that indicated the occurrence of extensive branch migration. Comparison with the crosslinked sample confirmed the effectiveness of the crosslinking in preserving structures created in the oocytes. Our results strongly support a resection–annealing mechanism of recombination in oocytes.

Key words: extrachromosomal recombination/nonconservative recombination mechanism/resection–annealing

Introduction

Homologous recombination occurs in many different cell types and in many classes of organisms. One tends to think first perhaps of meiotic recombination, because of its necessity for orderly chromosome segregation and its utility in genetic mapping (Hawley, 1988), but recombination is a consistent feature of mitotic cells too. In somatic cells, there is a strong association between homologous recombination and the repair of DNA damage, which has been demonstrated most convincingly in bacteria and in yeast (Friedberg, 1985). A detailed understanding of the molecular mechanisms involved in homologous recombination is both of general interest and critical in the design of efficient gene alteration protocols.

Homologous recombination mechanisms can be classified

as conservative or nonconservative depending on whether or not both copies of the interacting parental sequences are retained. Unlike meiotic recombination, which is conservative by necessity, the process in mitotic cells can proceed with either outcome. Somatic cells from a wide variety of organisms have been shown to catalyze non-conservative homologous recombination events between exogenous substrates (Lin *et al.*, 1984; Chakrabarti *et al.*, 1985; Folger *et al.*, 1985; Symington *et al.*, 1985; Carroll *et al.*, 1986; Seidman, 1987; Baur *et al.*, 1990). In yeast, nonconservative events have been reported to be involved in the repair of double-strand (ds) breaks induced by site-specific nucleases (Ruding and Haber, 1988; Ozenberger and Roeder, 1991; Plessis *et al.*, 1992).

As research on nonconservative recombination has progressed, molecular models have been created or adapted to account for the experimental findings. Two such models are illustrated in Figure 1. The resection–annealing or single-strand annealing mechanism is necessarily non-

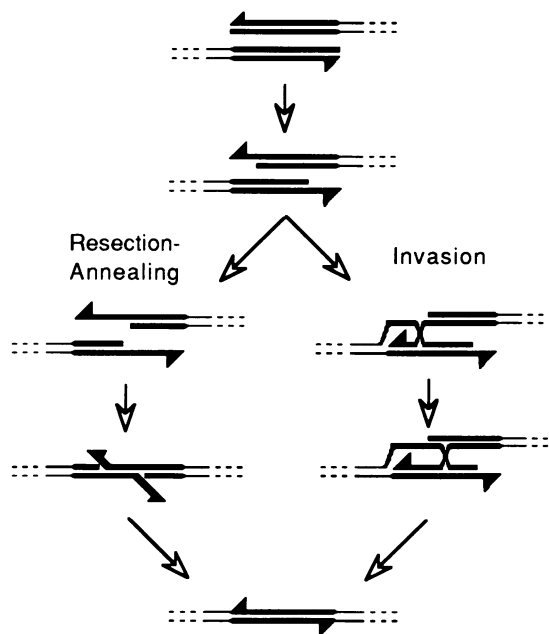


Fig. 1. Diagram of nonconservative recombination events between repeated DNA sequences illustrating two classes of mechanisms. Thick lines represent the repeats that support recombination; thin lines indicate unique sequences. Half-arrowheads denote 3' ends, while 5' ends are plain. The two interacting repeats may be on the same or different molecules. In the first step, 5' ends on both repeats are resected by 5'–3' exonuclease activity. In the resection–annealing model, nuclease action continues until complementary sequences are exposed as single strands; these anneal to form branched intermediates, which are subsequently resolved to completed junctions. In the invasion model, one ss tail invades homologous ds sequences in the other repeat, leading to the formation of intermediates with loops that can be converted to Holliday junctions and resolved by known activities (West, 1990).

conservative because one copy of the homology is degraded during the recombination process (Lin *et al.*, 1984; Maryon and Carroll, 1991b). The invasion mechanism is akin to models proposed for conservative processes in meiotic recombination, yeast transformation and bacterial recombination (e.g. Szostak *et al.*, 1983; Smith, 1988); thus, it is not obligatorily nonconservative, although it is unlikely that the reciprocal product would be recovered in events of the type illustrated in Figure 1. In these diagrams we show both pathways being initiated by 5'→3' exonucleolytic resection. This is justified by numerous earlier proposals regarding the importance of single strands (ss) in recombination and the observation that resection with this polarity is the principal fate of linear DNAs in yeast (White and Haber, 1990; Sun *et al.*, 1991) and in *Xenopus* oocytes (Maryon and Carroll, 1989).

Studies of nonconservative recombination have typically involved the rescue of functional genes (Lin *et al.*, 1984; Rubnitz and Subramani, 1984; Brouillette and Chartrand, 1987; Seidman, 1987; Rudin and Haber, 1988; Baur *et al.*, 1990; Kitamura *et al.*, 1990; Sugawara and Haber, 1992). Information on substrate requirements and product structures has been obtained, but direct evaluation of the mechanism by physical analysis of intermediates has generally been impossible. This limitation is overcome in the *Xenopus* oocyte system, where recombination intermediates can be detected and analyzed directly, due to the large amounts of injected DNA that are processed and the convenient time

course of recombination (Maryon and Carroll, 1989, 1991a,b). A single oocyte can recombine 10 ng of substrate in several hours. Furthermore, only homologous recombination occurs in oocytes (Carroll *et al.*, 1986; Grzesiuk and Carroll, 1987), whereas both homologous and non-homologous events are seen in mammalian cells (Roth and Wilson, 1988) and in *Xenopus* eggs (Goedecke *et al.*, 1992; unpublished results in our laboratory). Although oocytes are technically in meiosis, their large size is the result of the storage of materials for embryonic development (Gurdon and Wickens, 1983) and it is not surprising that they have recombination activities characteristic of somatic cells.

The evidence accumulated to date in our laboratory favors the resection–annealing mechanism of recombination over models based on strand invasion (Maryon and Carroll, 1991b; Jeong-Yu and Carroll, 1992). There are a number of earlier invocations of annealing mechanisms in other systems (Thomas, 1966; Cassuto and Radding, 1971; Lin *et al.*, 1984; Symington *et al.*, 1985), and supporting evidence continues to accumulate (Ozenberger and Roeder, 1991; Fishman-Lobell *et al.*, 1992). Nonetheless, we were concerned that intermediates generated by an invasion mechanism might have been unstable during our extraction procedures and thus have been overlooked. In this study we have addressed that issue by crosslinking the injected DNA in oocyte nuclei after incubation but prior to recovery. Candidate intermediates were then visualized in the electron microscope (EM) and characterized in detail by length

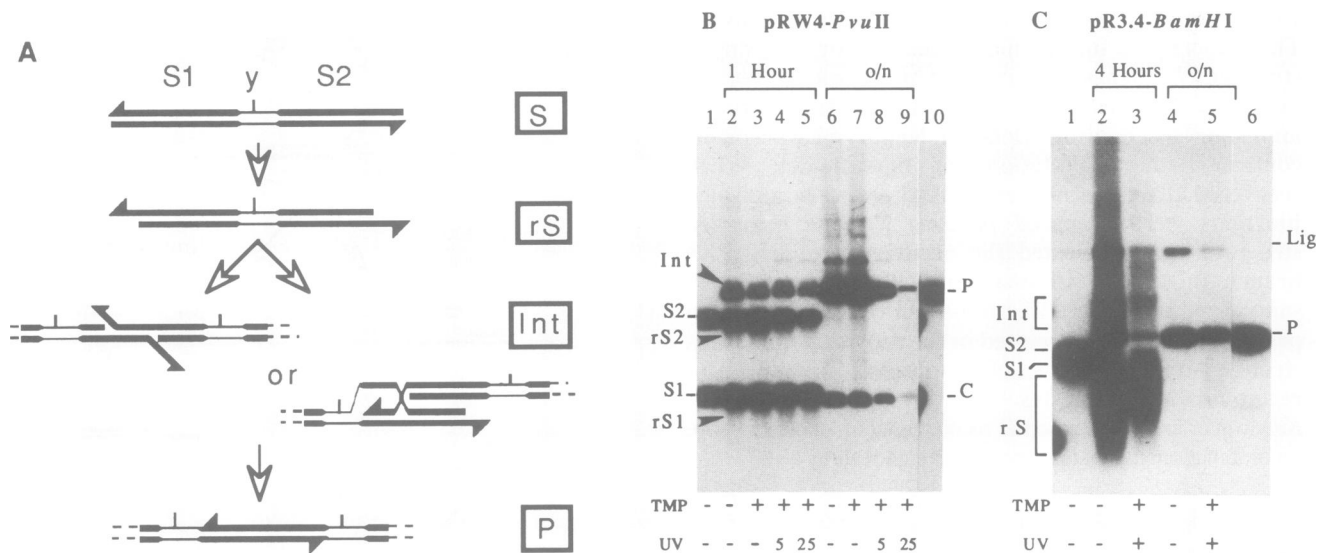


Fig. 2. Recombination of exogenous substrates in oocytes. (A) Diagram of the annealing and invasion mechanisms for linear DNA substrates with terminal direct repeats. Conventions are as in Figure 1. The short vertical line labelled *y* indicates the restriction site used for analysis after recovery from oocytes; S1 and S2 are the two substrate fragments produced by digestion at *y*. Following injection into oocytes, the substrate (S) is resected (rS) by 5'→3' exonucleolytic activity, intermediates (Int) are formed and products (P) are generated. In the Int and P diagrams, emphasis is placed on a single homologous overlap and neighboring sequences, and the remainder of each molecule is represented by dashed lines. (B) Southern blot analysis of pRW4 recombination in the presence of TMP. 7 ng of linear pRW4 and 1 ng of the circular control pHSS6 were injected into each oocyte and incubated for 1 h or overnight (o/n), as indicated. 10 ng of an uninjected sample (lane 1) and recovered DNAs from four oocytes in each condition (lanes 2–9) were digested with *PvuII* (*y* in panel A) prior to electrophoresis. Lane 10 contains 10 ng of pBR322 digested with *HindIII*. As indicated below the autoradiograph, the samples in lanes 2 and 6 were from injections without TMP. For the samples in lanes 3–5 and 7–9, the TMP concentration was maintained at 10 μ g/ml in the injection solution and the incubation medium. DNA was extracted from nuclei without irradiation (lanes 3 and 7) or with 5 min (lanes 4 and 8) or 25 min (lanes 5 and 9) UV irradiation. The positions of substrate (S1, S2), product (P) and pHSS6 fragments (C) are indicated. Beside lane 2, arrowheads show the positions of recombination intermediates (Int) and resected substrates (rS1 and rS2). (C) Southern blot analysis of pR3.4 recombination. 5 ng of linear pR3.4 was injected into each oocyte without (lanes 2 and 4) or with (lanes 3 and 5) TMP and incubated for the times indicated. The nuclei containing TMP were UV irradiated for 25 min. Before electrophoresis, the samples were digested with *BamHI* (*y* in panel A). DNA extracted from two nuclei was loaded in lanes 2 and 4, while DNA extracted from four nuclei was loaded in lanes 3 and 5. The positions of substrate fragments (S1, S2), resected substrates (rS) and products (P) are shown. The broad smear of intermediates is indicated (Int), as is the position of a band attributed to simple ligation of the original restriction ends (Lig). Hybridization in B and C was with a pBR322 probe.

measurements. As illustrated in Figure 1, intermediates of the resection–annealing and invasion pathways should be readily distinguished. Annealed junctions would have only ss branches, while invasion structures are characterized by internal loops. Only intermediates of the former type were seen, providing further confirmation of the resection–annealing mechanism.

Results

Conditions for psoralen crosslinking

The aim of this study was to visualize and analyze the structures of intermediates in oocyte recombination using EM. To ensure that what we observed was representative of what was actually present in the oocytes, and not a result of *in vitro* branch migration, we injected and incubated the DNA as usual, then crosslinked the species present with a psoralen derivative (4,5',8-trimethylpsoralen; TMP) before extraction. We first checked that co-injection of TMP (but without irradiation and crosslinking) did not alter the progress of the recombination reaction; we then found incubation times that maximized the amounts of recombination intermediates that were present; we determined irradiation conditions that led to efficient crosslinking of injected DNA in dissected oocyte nuclei after incubation and we established procedures for preparing these samples for examination by EM.

Conditions for TMP crosslinking were first determined

using linear pRW4 (Maryon and Carroll, 1989), which is a substrate used in many of our earlier studies. This plasmid has terminal direct repeats of 1.25 kb; its recombination is illustrated schematically in Figure 2A for both the resection–annealing and invasion mechanisms. In Figure 2B, a Southern blot analysis of pRW4 recombination in the absence and presence of TMP is shown. After incubation in the oocytes but prior to analysis by electrophoresis, the DNA was digested with *Pvu*II (shown as γ in Figure 2A) which has a unique site in the non-repeated portion of pRW4. *Pvu*II cuts the linear substrate into two fragments (S1 and S2, respectively) and generates a unique diagnostic fragment (P) from recombination products, whether they are produced by intra- or intermolecular events.

After 1 h of incubation in oocyte nuclei, both substrate and product bands were visible (Figure 2B). In addition, the molecules that migrated more quickly than the substrate bands correspond to partially resected substrates (rS1 and rS2), and the molecules that migrated more slowly than products correspond to recombination intermediates (Int) (Maryon and Carroll, 1991b). After overnight incubation, product molecules (P) were the major species; the larger substrate band (S2) was essentially absent, while the band running with S1 (C in Figure 2B) was actually derived from pHSS6, a circular plasmid that was co-injected as a recovery control, but did not participate in the recombination reaction (Carroll *et al.*, 1986; Jeong-Yu and Carroll, 1992a,b).

The experiment presented in Figure 2B shows that the

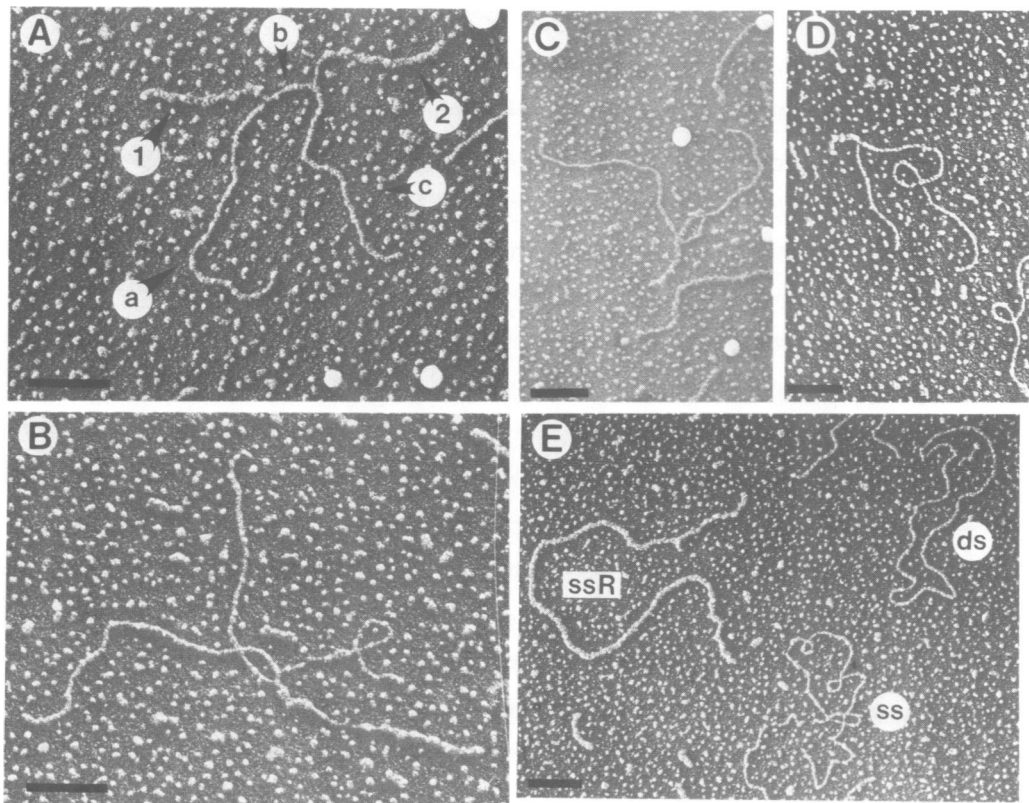


Fig. 3. Electron micrographs of branched junctions from crosslinked pR3.4. Two 2-branched junctions (A and B) and two 1-branched junctions (C and D) are shown. After 4 h in oocytes and 25 min of UV crosslinking, the DNA was digested with *Bam*HI and coated with RecA protein in preparation for EM. In these conditions, ds DNA appears as a smooth filament, ss coated with RecA as a thick filament, and uncoated ss as a thin and irregular filament. This is illustrated in panel E which shows examples of each of the standard molecules used: ds, M13mp19 open circular ds; ss, M13mp19 linear ss; ssR, M13mp19 linear ss coated with RecA protein. In A, C and D, all the ss branches were completely coated with RecA protein, while those in B were incompletely coated. In panel A, the labels a, b, c, 1 and 2 indicate the different segments of the junction as identified in Figure 5. The bars represent 0.2 μ m.











	Structures			Frequencies (%)			
	Observed	Interpreted	Named	cross linked n=56	non-crosslinked N1 n=175	N2 n=59	<i>in vitro</i> n=42
Junctions			2-branched	63	61	42	93
			1-branched	37	39	58	7
Branches			I branch	n=89 94	n=281 59	n=84 76	n=81 54
			V branch	3	32	14	38
			Long I branch	3	9	10	8

Fig. 4. Structure and frequency of the figures observed. The frequencies are expressed as percent of the total number of junctions (top area) or as percent of the total number of branches (lower area). The frequencies of 1- and 2-branched junctions were determined irrespective of the structure of the branches. N1 is a non-crosslinked sample from the same experiment as the crosslinked sample, while N2 is from a separate experiment. The *in vitro* sample was prepared by controlled digestion with T7 gene 6 exonuclease (see text).

presence of TMP in the oocytes did not alter the kinetics of the recombination reaction. The same electrophoretic profiles were obtained without TMP (lanes 2 and 6) and when TMP was co-injected with the DNA, but not irradiated (lanes 3 and 7). Samples from some of the TMP-containing oocytes were crosslinked after incubation by UV irradiation of manually dissected nuclei before the DNA was extracted, digested and analyzed (lanes 4, 5, 8 and 9). The same species were present, but there was a slight reduction in the mobility of the irradiated DNA (more visible after overnight incubation; compare lanes 8 and 9 with lane 7), indicating that crosslinking had occurred (Cech, 1981). The difference in migration was more evident when the time of UV irradiation was longer (lane 9), indicating that a higher density of crosslinks was obtained. A reduction in signal intensity after crosslinking was often observed, possibly due to decreased efficiency of transfer and hybridization of crosslinked DNA.

For visualization in the EM, we chose a substrate with longer homologous sequences, which should make recombination intermediates more abundant and their unique features easier to measure accurately. Linear pR3.4 is 7.80 kb long and carries terminal direct repeats of 3.41 kb. An analysis of the recombination of linear pR3.4 in oocytes is presented in Figure 2C. Before electrophoresis the DNA was cut with *Bam*HI (y in Figure 2C), which yields two substrate fragments of 3.76 and 4.04 kb (S1 and S2) and a product fragment of 4.36 kb (P). After overnight incubation in the oocytes, product molecules were the major species. The band labelled Lig in Figure 2C was 7.80 kb in size and was sensitive to *Apa*I digestion; it is the result of the ligation of the GC-rich *Apa*I sticky ends of the original

substrate (R.J.Dawson and D.Carroll, in preparation). After 4 h of incubation, substrates, partially resected substrates, intermediates and products were all present. The overall rate of recombination was slower than in the case of pRW4, and the smears of resected substrates and intermediates were more extensive. The intensities of these smears indicated that intermediate species would be relatively abundant and easy to find in the EM.

As already noted for pRW4, the only detectable difference between the unirradiated control and the crosslinked DNA was a slight decrease in mobility (compare lane 4 with lane 5 in Figure 2C). To determine the density of crosslinks in pR3.4, an aliquot of the sample shown in lane 3 of Figure 2C was analyzed by EM under totally denaturing conditions (see Materials and methods). We estimated that the minimum density of crosslinks was 1 per 190 bp (data not shown). If the crosslinks were evenly distributed, there would be 18 crosslinks in the 3.41 kb homology of pR3.4, which should be adequate to limit branch migration of an invasion structure present anywhere in the homology.

Molecules observed by EM in a partially recombined sample

A sample of pR3.4 DNA that had been incubated in oocytes for 4 h (lane 3 in Figure 2C) was crosslinked, extracted, cut with *Bam*HI and prepared for EM. In order to visualize intermediates of all types, we did not attempt any fractionation prior to EM. To increase the contrast of ss DNA, the sample was coated, prior to spreading, with RecA protein under conditions in which the protein binds only to ss DNA and does not promote homologous

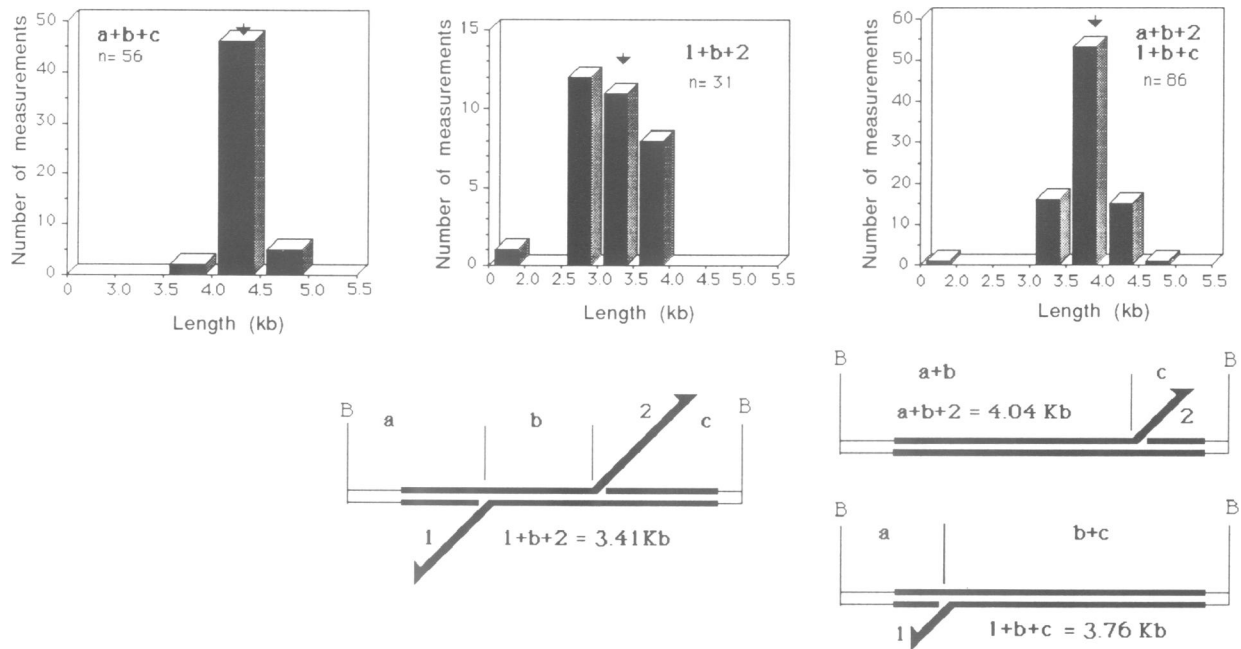


Fig. 5. Size distributions of diagnostic segments of branched junctions from the crosslinked pR3.4 sample. Interpretive diagrams of 2- and 1-branched structures are shown below the histograms, indicating the segments measured separately. Conventions are as in Figure 1. The letters a, b and c denote ds regions of junctions while the numbers 1 and 2 represent the ss branches. The position of cleavage by *Bam*HI is indicated by B. Measurements were made on photographs like those shown in Figure 3. In each histogram, the segments measured and the number of independent measurements are given. Vertical arrows indicate the expected sizes. In the middle and right histograms, the single outlying value (which came from the same molecule in the two cases) was omitted from the calculation of average lengths (Table I). It may have resulted from a nonspecific break in one 3'-ending strand.

recombination (see Materials and methods). In these conditions, ss DNA coated with RecA appears as a thick filament while ds DNA is thin and smooth (Dunn *et al.*, 1982). Three different molecules were included as size standards and to aid the recognition of ds and ss DNA: M13 open circular ds, M13 linear ss coated with RecA and uncoated M13 linear ss (see Figure 3E). The latter was included because the coating with RecA was never complete in our experiments.

All molecules observed in this sample could be structurally classified into four categories: linear fully ds, linear ds with an ss tail, branched molecules and uninterpretable aggregates. Molecules with internal loops were not detected. The frequency of each species was determined both by counting during EM observation and by classification from photographic prints.

38% of the species observed were fully ds, and measurements showed that they corresponded in size to intact substrates, recombination products and products of direct *Apa*I end ligation (data not shown). 45% of the structures were linear ds with one ss tail. Measurements made on these molecules indicated that they corresponded to resected substrate fragments (data not shown). About 11% of the observed species were branched; these are analyzed in detail below. Finally, the remaining 6% were small aggregates, mainly appearing as rosettes, which may be artifacts of the EM preparation.

Structures of branched molecules from a crosslinked sample

In the *Bam*HI-cut crosslinked sample, a large majority (83%) of the branched molecules had only ss branches. Some examples are shown in Figure 3. As detailed in this section,

their features correspond to the expectations of the resection–annealing mechanism. The remaining 17% showed branches with both ds and ss regions and are analyzed in a later section. The nomenclature used to describe the major types of branched molecules, which we interpret as unfinished recombination junctions, is summarized in Figure 4. Ds molecules were seen to have either two or one branch points from which ss emerged (2-branched and 1-branched junctions). At each of these branch points, one (I branch) or two (V branch) ss protrusions were present. When the ss was longer than the distance from the branch point to the nearer end of the duplex, this was termed a long I branch. As indicated in Figure 4, the majority of junctions seen in the crosslinked sample were 2-branched; and nearly all the branches were simple I's. Examples of 2-branched and 1-branched junctions with simple I branches are shown in Figure 3. In these photographs, the distinction between ds regions and RecA-coated ss is evident.

Length measurements were performed on 56 well separated 1- and 2-branched molecules and converted to kb by comparison with the appropriate M13 standards. Histograms of the lengths and interpretive diagrams are given in Figure 5. Population averages are collected in Table I; they correspond to the predictions of the resection–annealing model.

The total duplex length ($a + b + c$ in Figure 5) was 4.27 ± 0.18 kb, which is very close to the expected value of 4.36 kb. This is a strong prediction of an essentially any homology-dependent mechanism and justifies our interpreting these branched structures as junctions in recombination intermediates. It is also reasonable to identify these structures with the molecules migrating more slowly

Table I. Sizes of diagnostic segments

Segments	Expected size	Sample		
		Crosslinked	Non-crosslinked (sample N2)	<i>In vitro</i>
a + b + c	4.36	4.27 ± 0.18 (n = 56)	4.27 ± 0.16 (n = 53)	4.33 ± 0.30 (n = 42)
1 + b + 2	3.41	3.17 ± 0.36 (n = 30)	3.43 ± 0.40 (n = 15)	3.44 ± 0.57 (n = 13)
a + b + 2	4.04	3.71 ± 0.49 (n = 86)	3.92 ± 0.43 (n = 66)	3.92 ± 0.47 (n = 50)
1 + b + c	3.76			

The overall lengths (a + b + c) were determined for all branched junctions. The sizes 1 + b + 2, a + b + 2 and 1 + b + c were determined using only I branches. All sizes are given in kb ± the sample standard deviation.

Table II. Extent of resection

Type of molecules	Sample		
	Crosslinked	Non-crosslinked (sample N2)	<i>In vitro</i>
Resected substrates	1.0 ± 0.5, n = 68, 9% > 1.7	1.0 ± 0.5, n = 60, 5% > 1.7	nd
Annealed junctions	2.0 ± 0.6, n = 60, 63% > 1.7	2.5 ± 0.6, n = 28, 89% > 1.7	2.5 ± 0.4, n = 23, 100% > 1.7

All sizes are given in kb ± the sample standard deviation. The number of measurements is indicated for each sample, as is the percent of resection lengths greater than 1.7 kb. nd = not determined.

than products in electrophoresis (Figure 2C); they should be retarded both by their excess mass and their branched configuration.

Because the branched junctions had the general appearance of the proposed intermediates of the resection–annealing model, we analyzed other lengths to compare with predictions of that mechanism. In oocytes, only 5'-ending strands are resected, while 3' ends remain intact (Maryon and Carroll, 1989, 1991a,b). Therefore, the distance from the end of one ss tail through the intervening ds segment to the end of the other ss tail (1 + b + 2 in Figure 5) should equal the size of the initial homologous overlap. This value was calculated for 31 2-branched junctions to be 3.17 ± 0.36 kb (Table I). This is close to the expected value of 3.41 kb. The measured length may be slightly diminished by fixation of intrastrand duplex regions in the ss branches by psoralen crosslinking.

When only one branch was visualized (Figure 3C and D), we imagine that the other branch was already assimilated, and possibly ligated, at the other end of the overlap. Depending on which end remained, two lengths are predicted for the sizes a + b + 2 and 1 + b + c, but the expected values of 3.76 and 4.04 kb are not distinguishable in these measurements. Measurements of a + b + 2 and 1 + b + c (right histogram in Figure 5) were obtained from 21 1-branched junctions, from 31 2-branched junctions (2 values each), and from 3 I branches of 2-branched molecules which also had a V branch. The average length for a + b + 2 and 1 + b + c was close to the expected value (Table I). The large standard deviation may reflect the fact that two different actual lengths were included.

Lengths of resection

We hoped to determine how much exonuclease action was required to initiate formation of recombination intermediates by measuring the extent of resection for both resected

substrate fragments and branched recombination junctions. The values are reported in Table II. As noted above, a substantial number of *Bam*HI fragments having a ss tail and an overall length corresponding to intact substrate fragments were seen. There was quite a broad range of tail lengths, but only a few molecules (9%, Table II) had ss tails more than half the length of the homology; this suggests that molecules with more extensive resection were rapidly converted to recombination junctions.

In 2-branched junctions, the extent of resection on each strand can be calculated as the distance from the end of one ss branch, through the ds segment, to the base of the second branch (1 + b and b + 2 in the diagram in Figure 5). Longer resection tracks were observed in the intermediates than in the resected substrates (Table II). The large standard deviation associated with the resection values reflects a broad distribution of lengths and indicates that, within the population, there were junctions at different stages of the recombination process. This asynchrony is consistent with the broad smear attributed to intermediates in electrophoresis (Figure 2C). Most of the resection lengths were > 1.7 kb (Table II), indicating that approximately half of the homologous overlap must be resected in order to form annealed intermediates.

Junction structures without crosslinking

To verify the effectiveness of the TMP crosslinking, two non-crosslinked samples were also analyzed: one (N1) from the same experiment as the crosslinked sample, but from injections without psoralen (Figure 2C, lane 2), and the other (N2) from a separate experiment. The junctions seen in these two samples were generally very similar. The most obvious difference from the crosslinked sample was the presence of more V branches and long I branches in N1 and N2 (Figure 4). Photographs of such structures are shown in Figure 6A and B. This result was expected, since we believe that V

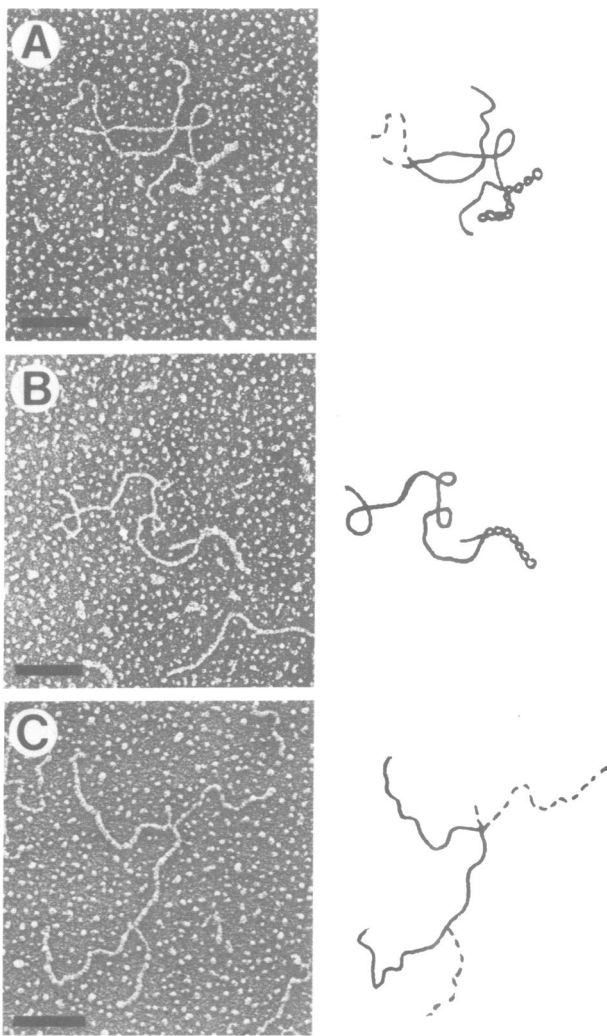


Fig. 6. Electron micrographs of junctions with V branches (A and C) and a long I branch (B). The photographs in A and B were from the non-crosslinked N2 sample after a 4 h incubation in oocytes. The molecule in C was from annealed junctions made *in vitro* with T7 gene 6 exonuclease. In the explanatory drawings, plain lines represent segments interpreted as ds DNA, broken lines indicate ss DNA, and strings of open circles represent ss DNA coated with RecA protein. The bars represent 0.2 μm .

and long I branches are derived from simple I branches by branch migration. The differences from the crosslinked sample show that the crosslinking was effective in preventing the isomerization of junctions that occurred readily in its absence.

Detailed length measurements were made on sample N2. The lengths of the diagnostic segments were all in excellent agreement with the predictions of the resection–annealing model (Table I). In N2, the average junction was closer to completion than in the crosslinked sample or N1. This is reflected in the greater proportion of 1-branched junctions (Figure 4) and in the greater extent of resection in annealed junctions (Table II). We do not know the reason for this difference, but it does not detract from the overall structural similarity of the molecules observed in the independent injections.

If the V and long I branches arose by isomerization of simple I branches, some aspects of their structures are predictable. Although one ss of a V branch should still

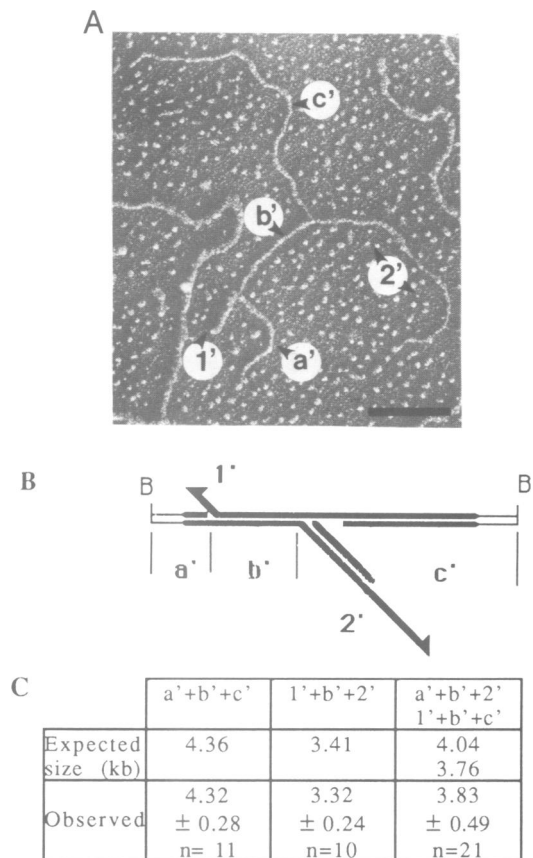


Fig. 7. Rare junctions with ds branches. (A) Electron micrograph of a molecule from the same sample as those in Figure 3. The labels a' , b' , c' , $1'$ and $2'$ indicate the different segments of the molecules as interpreted in B. The branch $1'$ was completely coated with RecA protein, while the ss portions of $2'$ and c' were not. The bar represents 0.2 μm . (B) Interpretive diagram showing annealing of a ss tail from one molecule ($1'$, b' and c') in a ss gap of another (a' , b' and $2'$). As in Figure 1, thick lines represent homologous sequences, half-arrowheads denote 3' ends and 5' ends are plain. Bs at the ends of the structures indicate sites of cleavage by the analytical enzyme, *Bam*HI. (C) Measured lengths are given and compared with the expected values for the hypothesized structure.

represent an original 3' end and therefore the end of the homologous overlap, we could not determine independently which ss that was. However, it was true for all V structures that one of the ss branches had a length that corresponded to this expectation when used to calculate $1 + b + 2$ or $a + b + 2/1 + b + c$ (data not shown). In long I branches, the ss was interpreted as a 5'-ending strand that was displaced by branch migration to the end of the homology. Although all lengths including these ss branches are expected to be variable, the ds lengths from the branch point to the *Bam*HI site (corresponding to a and c in Figure 5) are predictable: 0.35 kb at one end and 0.62 kb at the other end. The two ends cannot be distinguished experimentally, but the average value of all such terminal ds regions was 0.35 ± 0.20 kb ($n = 11$) in long I structures from N2, in reasonable agreement with expectation.

Annealed junctions made *in vitro*

As further confirmation of our interpretations of the structures observed by EM, we prepared annealed junctions *in vitro*. Approximately 2200 nucleotides were removed from each end of linear pR3.4 with T7 gene 6 exonuclease

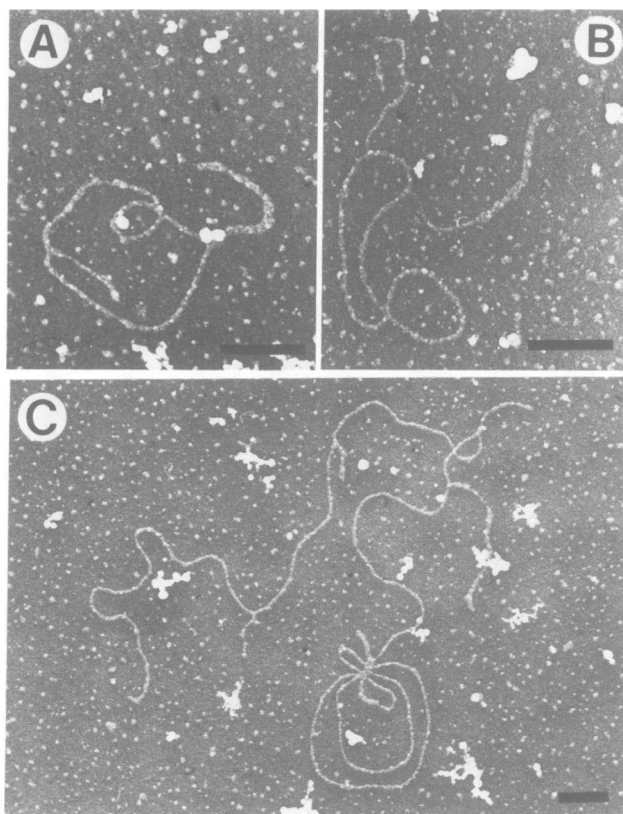


Fig. 8. Electron micrographs of branched junctions in undigested DNA. Intermediates from intra- (A and B) and intermolecular (C) recombination events are shown. These pictures were taken from sample N2, extracted after 4 h incubation of linear pR3.4 in the oocytes. The DNA was coated with RecA in preparation for EM, but was not digested with *Bam*HI. The coating with RecA was incomplete; for example, notice that the inner branch of the molecule in A is not coated while the exterior branch is. The dense, irregular material in the background is from the uranyl acetate stain. The bars represent 0.2 μ m.

(see Materials and methods), which, like the *Xenopus* exonuclease, degrades 5' \rightarrow 3' on ds DNA. These molecules were annealed, then digested with *Bam*HI and prepared for EM. 72% of the molecules appeared branched, and 93% of those were 2-branched (Figure 4). Nearly half the branches were Vs and long I's (Figure 4), as expected for junctions that were free to isomerize by branch migration. One example is shown in Figure 6C. Measurements performed on these *in vitro* junctions agreed with the expectations (Table I).

Because all molecules were treated simultaneously with the T7 gene 6 exonuclease in conditions of enzyme excess, they should all have been resected to the same extent and have essentially the same structure. In fact, the calculated resection length (1 + b and b + 2) was in good agreement with expectation (Table II), and the relatively small standard deviation indicates that nearly synchronous resection was achieved. Six long I branches were analyzed in this sample, and the lengths of the terminal ds segments were 0.40 ± 0.05 kb, again matching expectation.

Minor branched structures

As mentioned earlier, 17% of the branched molecules observed in the crosslinked sample had a structure different from the junctions just described. Their incidence was 14%

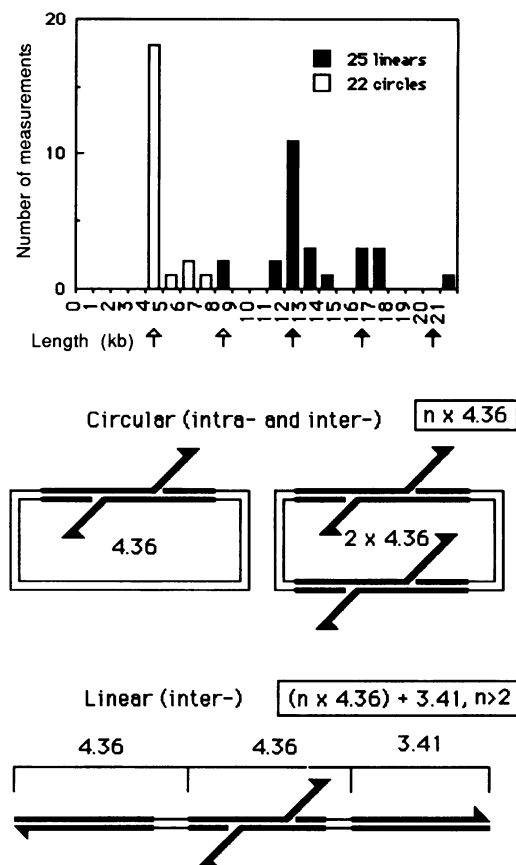


Fig. 9. Size distribution of ds backbones of undigested branched junctions like those of Figure 8. The number and configuration (circular or linear) of the measured molecules are indicated. The diagrams below the histogram show the size predictions for both intra- and intermolecular recombination events. Vertical arrows under the histogram indicate the expected positions for the peaks (open arrows: circular; closed arrows: linear). The three circles with anomalous sizes of 6–7 kb had branches that were less obvious than usual, and they could correspond to M13 ds circular control molecules with a branch artificially created by the EM background or by folding of the molecule. The linear ds lengths (8–9 kb) that did not fit with the predictions could be the result of random ds breaks.

in the non-crosslinked control from the same injections. An example of this type of molecule is presented in Figure 7A. These structures are 2-branched, but have the characteristic feature that there are ds regions in all three segments emerging from one of the branch points. There was usually a ss region at the end of one of these ds branches and adjacent to the branch point on another of them. A diagram showing our interpretation of the strand composition of these structures is presented in Figure 7B. As elaborated in the Discussion, such structures may have resulted from annealing at a gap or from DNA synthesis occurring on an ss branch of the usual type. We made length measurements on 11 molecules of this type from the crosslinked sample, where there was less chance of ambiguity due to isomerization. The measured values were in very good agreement with predictions based on the interpretation (Figure 7C).

The fact that the frequencies of this minor population of junctions were similar with and without crosslinking suggests that they were not created artifactually, either by crosslinking or by branch migration. There were many fewer such structures in N2, which was from an independent injection. The interpretation of this difference depends on the

mechanism by which these structures were formed (see above).

Inter- and intramolecular recombination events

When DNA recovered from oocytes is analyzed directly, without cleavage by an analytical enzyme before gel electrophoresis, there is evidence of both intra- and intermolecular recombination products (Maryon and Carroll, 1989, 1991b). We carried out an EM analysis of the non-crosslinked sample N2 of pR3.4, extracted after 4 h of incubation, without *Bam*HI treatment. Fully ds molecules and molecules with ss regions were observed. Both circular and linear molecules containing ss branches were seen (Figure 8). The circular molecules are believed to be the result of intramolecular recombination events, while linear molecules are the result of intermolecular events, as diagrammed in Figure 8.

Because oocyte recombination is nonconservative, the lengths of the ds backbones of these molecules should be equal to the lengths of product molecules. This distance was measured on 22 circular and 25 linear molecules containing branches (Figure 9). The sizes of the circles are expected to be $n \times 4.36$ kb, and the sizes of linear molecules ($n \times 4.36$) + 3.41 kb, with $n \geq 2$. The histogram shows that the molecules generally fell into the predicted size classes.

Discussion

The results reported in this paper strongly support the resection–annealing model of nonconservative recombination in *Xenopus* oocytes. Only branched molecules with structures consistent with the predictions for annealed intermediates were detected in psoralen-crosslinked samples. No internal loops were observed. Experiments with RecA-generated invasion structures (McEntee *et al.*, 1979; Shibata *et al.*, 1979) indicate that putative invasion loops could have been detected using the EM technique we employed, if they had been present.

Both the abundance and the general appearance of the branched structures observed by EM correspond to features of the molecules previously interpreted as recombination intermediates by biochemical analysis (Maryon and Carroll, 1991b). They represent ~10% of all molecules seen by EM, which mirrors the intensity of the smear migrating more slowly than product in a Southern blot analysis (see Figure 2C). They have a ds length equal to that of products, with ss branches as expected for a heteroduplex junction between two substrates. This family of structures is consistent with the electrophoretic mobility of the intermediates in non-denaturing gels (slower than product due to the presence of branches and broadly distributed because of the variable lengths of those branches) and with their strand composition as determined by two-dimensional gel electrophoresis (Maryon and Carroll, 1991b). When the DNA was not digested with *Bam*HI before analysis, branched circular and linear ds molecules were observed (Figure 8). The sizes of the ds backbones of these molecules were again in agreement with predictions. Because the same types of structures (i.e. ss branches) were found on both circular and linear molecules, we conclude that intra- and intermolecular recombination proceed via the same mechanism.

Detailed length measurements on the branched junctions confirmed the predictions of the resection–annealing model

in all respects. The fact that the distance between ss ends in 2-branched junctions matched closely the length of the homologous overlap indicates that only one strand is degraded during recombination. This accords well with previous results, which showed that the ss branches in annealed junctions were largely intact 3'-ending strands (Maryon and Carroll, 1991b), which is expected from the 5'→3' polarity of the oocyte exonuclease (Maryon and Carroll, 1989). We have made no special effort to distinguish 5' and 3' ends in the EM, but we can derive some information from the appearance of RecA-coated ss in I branches. When such branches were incompletely coated, the proximal portion in the majority of them was uncoated and the distal portion was fully coated. This is consistent with random internal nucleation of RecA binding, then 5'→3' polymerization (Register and Griffith, 1985) on ss branches ending 3'.

When the DNA was not crosslinked prior to extraction, ss branches interpreted as 5'-ending were observed (i.e. in V and long I branches). This is consistent with previous work which indicated that some 5'-ending strands were sensitive to S1 nuclease (Maryon and Carroll, 1991b). There were very few V and long I branches in the crosslinked sample. This suggests that they were not present in the oocytes, but were produced from simple I branches by branch migration during isolation. Therefore, junctions with 5'-ending ss branches are not intermediates in the recombination pathway.

We are aware that junctions with 3'-ending ss branches can be derived from invasion structures by branch migration and continued exonuclease action (Maryon, 1990). They must arise, however, from 5'-ending V or long I branches, and there is no obvious reason why this should be the favored outcome, particularly in the crosslinked sample. Furthermore, the absence of invasion loops discourages attempts to account for the observations by elaborations on an invasion mechanism.

The ds branched structure observed in a minority of molecules (Figure 7) may have arisen from exonuclease initiation at an internal nick and annealing of a ss tail in the resulting gap. Alternatively, it may have been derived by priming of DNA synthesis (Cortese *et al.*, 1980) somewhere on one of the 3'-ending ss branches of a normal annealed intermediate. It is also conceivable that the heteroduplex part of this junction has a three-strand structure rather than being duplex DNA. These two DNA conformations are not distinguishable by the EM technique used. Triplex intermediates have been observed in homologous pairing reactions catalyzed by RecA (Hsieh *et al.*, 1990; Rao *et al.*, 1991) and they can be crosslinked by psoralens (Umlauf *et al.*, 1990). We cannot formally exclude the possibility of a triplex structure as an intermediate in oocyte recombination, but there is little evidence to suggest its participation. One might expect triplexes to be preserved by psoralen crosslinking, but to be unstable without crosslinking. If that were true, the apparent heteroduplex region (b in Figure 5) should be longer in the crosslinked than in the non-crosslinked (N1) sample, and the ss branches should be shorter. This was not observed (data not shown). In the absence of direct evidence for triplexes, we adopt a simpler version of the resection–annealing mechanism.

Our current view of the mechanism of homologous recombination in *Xenopus* oocytes is summarized in Figure 10. The majority of the molecules follow a pathway (left side, Figure 10) in which one strand at each end of the linear

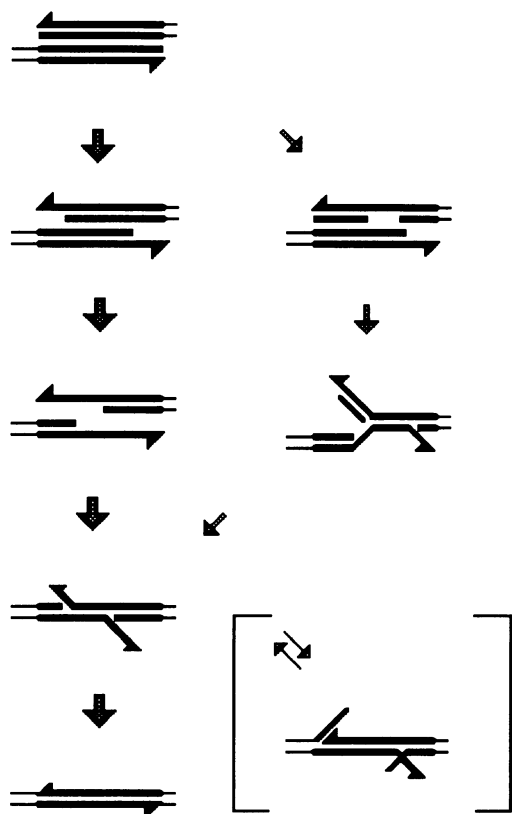


Fig. 10. The resection–annealing mechanism, illustrated for one junction between two substrates. Conventions are as in previous figures. The straight vertical pathway on the left shows the most common steps in oocyte recombination. On the right are the steps that occur, less frequently, when ss gaps participate in recombination. The bracketed structure at the bottom right shows the isomerized junction structures that are in equilibrium with branches formed in oocytes in the absence of crosslinking. See text for details.

substrate is resected by 5'→3' exonuclease activity, until complementary sequences in the two homologous repeats are exposed. These sequences anneal, giving rise to the branched intermediates visualized by EM. Further resection of the redundant 5'-ending strands allows assimilation of the 3' branches, and ligation completes the formation of covalently-closed products. Less frequently (Figure 10, right), the 5'→3' exonuclease may act at a nick; annealing of the sequence present in the resulting ss gap with a complementary sequence present in a ss tail could give rise to annealed intermediates with partially ds branches. V and long I branches with 5'-ending ss (Figure 10, lower right, in brackets) are formed only by isomerization during extraction.

Both electrophoretic data (Maryon and Carroll, 1991b; Jeong-Yu and Carroll, 1992b) and our EM measurements suggest that the rates of formation and resolution of recombination intermediates are governed by the rate of the 5'→3' exonuclease. First, there is a broad distribution of ss tail lengths on substrate fragments that have not formed annealed junctions (Table II), but very few of those tails are longer than half the homologous overlap. Conversely, the lengths of resection determined for annealed junctions are also varied, but are on average greater than half the overlap (Table II). This suggests that molecules resected deeply enough to expose homologous ss readily find each other and

anneal. The resulting junctions would thus usually form near the middle of the overlap. While this may be true, there is no necessary correspondence between the amount of resection of the interacting parental homologues, because we found that the lengths of the individual ss branches in 2-branched intermediates were not highly correlated (data not shown). Finally, we have not seen intermediates in pR3.4 recombination with ss gaps beyond the end of the homologous overlap. This indicates that completion of the junction by ligation (possibly in conjunction with DNA synthesis) occurs rapidly after removal of the redundant strand by the exonuclease and assimilation of the branched 3' end.

A pathway of non-conservative recombination very similar to that in *Xenopus* oocytes has been proposed to account for repair of some ds breaks in yeast (Ozenberger and Roeder, 1991; Fishman-Lobell *et al.*, 1992). In that organism ds ends are also subject to the action of a 5'→3' exonuclease (White and Haber, 1990), and it is quite plausible that annealed intermediates are formed, although there is presently no direct evidence for their existence.

In cultured animal and plant cells, extrachromosomal recombination is efficient and predominantly nonconservative (Subramani and Seaton, 1988). Existing data, although indirect, are in accord with the resection–annealing mechanism (Lin *et al.*, 1984). Gene targeting in mammalian cells appears to proceed via a conservative mechanism (Pennington and Wilson, 1991); but, in contrast to extrachromosomal events, targeting occurs only at low frequency. We expect that continuing investigation of homologous recombination in oocytes will provide insights applicable to many other systems, and perhaps guide attempts to make the efficient nonconservative recombination mechanism effective at chromosomal sites.

Materials and methods

DNA substrates

The substrates for homologous recombination were the plasmids pRW4 and pR3.4, both of which are partial dimers of pBR322. pRW4 has 1.25 kb direct repeats separated by an *Xho*I site (Maryon and Carroll, 1989). pR3.4 was constructed from pRDK41, a mutant dimer of pBR322 (Doherty *et al.*, 1983) and is 7.80 kb long, including a tandem repeat of 3.4 kb in which the copies are separated by an *Apa*I site (R.J.Dawson and D.Carroll, in preparation). The unique sequence of pR3.4 contains the *Bam*HI restriction site used for analysis. pHSS6 (Seifert *et al.*, 1986) was coinjected with pRW4 as a recovery control (Jeong-Yu and Carroll, 1992a,b).

Injection and recovery of DNA

Our procedures were largely similar to those previously described (Maryon and Carroll, 1989). Before injection, pRW4 was digested with *Xho*I and pR3.4 was digested with *Apa*I, following the manufacturer's specifications (Bethesda Research Laboratories, Inc., Rockville, MD). The DNA was extracted with phenol:chloroform:isoamyl alcohol (25:24:1 v/v), and then twice with ether, followed by precipitation with 2.5 vol of ethanol. The DNA was redissolved in 15 mM Tris–HCl, pH 7.5, 88 mM NaCl at a concentration of 250–500 µg/ml, and 20 nl of this solution was injected into the nucleus of each oocyte.

The injected oocytes were incubated at 19°C in OR-2 (Wallace, 1973) for various periods of time. Nuclei were manually dissected and transferred to 0.1 M glycine, pH 9.6, 0.2 M NaCl, 1 mM EDTA. DNA was extracted as described by Maryon and Carroll (1989), except for the addition of a 10 min digestion with RNase A (10 µg/ml) followed by extraction and precipitation as described above. Glycogen (Boehringer Mannheim Biochemical, Indianapolis, IN) was used as a carrier instead of tRNA during the ethanol precipitation. These steps were taken to eliminate RNA background in the EM.

Psoralen crosslinking of the DNA in oocytes

4,5',8-Trimethylpsoralen (TMP) (Trioxsalen, Sigma Chemical Co., St Louis, MO), at a final concentration of 10 µg/ml, was injected into the oocyte nuclei along with the linear substrate, which was at 250 µg/ml. The oocytes were incubated in OR-2 containing 10 µg/ml of TMP. After dissection, the nuclei were transferred to ice-cold extraction buffer containing 10 µg/ml of TMP in a 96-well flat-bottom plate (Corning, Corning, NY). Approximately 130 nuclei were placed in a total volume of 50 µl. One microliter of TMP, at 500 µg/ml in ethanol, was added and the plate was irradiated for 5 min on a Chromato-Vue Transilluminator (UV Products, Inc., San Gabriel, CA; peak emission at 365 nm). The addition of TMP and irradiation were repeated four times. DNA was extracted as described above, then digested with *Bam*HI, extracted with phenol:chloroform:isoamyl alcohol and ether, and ethanol precipitated. The same crosslinked DNA was used for analysis by gel electrophoresis and blot hybridization, for estimation of the density of crosslinks by EM, and for visualization of recombination intermediates by EM.

Gel electrophoresis and blot hybridization

Gel electrophoresis was in 1% agarose. The DNA was transferred to a Zetaprobe nylon membrane (Bio-Rad Laboratories, Richmond, CA) in 0.4 M NaOH, using a vacuum blotting system. Transfer was preceded by 15 min of depurination in 0.25 M HCl. The filters were hybridized using the Church protocol (Church and Gilbert, 1984) with a random-primed pBR322 probe (Feinberg and Vogelstein, 1983).

Annealed junctions made in vitro

*Apa*I-cut pR3.4 (100 µg/ml) was incubated at room temperature with 5000 U/ml T7 gene 6 exonuclease (US Biochemical Corp., Cleveland, OH), in 50 mM Tris-HCl, pH 8.0, 5 mM MgCl₂, 20 mM KCl, 5 mM 2-mercaptoethanol. After 2 min, aliquots were removed approximately every 40 s and quenched with 3 vol of ice-cold buffer (10 mM Tris-HCl, pH 8.0, 20 mM EDTA). The reaction mixtures were extracted and precipitated as above and the pellets were dissolved in TE buffer (10 mM Tris-HCl, pH 8.0, 1 mM EDTA). No separate annealing step was performed. The rate of the resection was estimated at 500 nucleotides per end per minute by size determination using agarose gel electrophoresis after treatment of the DNA with 4 U S1 nuclease (Bethesda Research Laboratories) for 20 min at room temperature, in 50 mM sodium acetate, pH 4.5, 150 mM NaCl, 0.5 mM ZnSO₄. The sample analyzed by EM had been treated with T7 gene 6 exonuclease for 4 min and 10 s; it was digested with *Bam*HI in a low salt (buffer L, Boehringer Mannheim Biochemical) before preparation for EM.

Electron microscopy

Size standards. We used both ds and ss forms of M13mp19, which is 7.25 kb long, as size standards. Ds open circles were prepared by treatment of supercoiled ds M13mp19 with DNase I (5 µg/ml), in the presence of 500 µg/ml ethidium bromide, for 30 minutes at 37°C (Gruss *et al.*, 1990). Ss linear DNA was prepared by *Eco*RI digestion of M13mp19 ss circles hybridized with an oligonucleotide (RD 20 Primer, New England Biolabs, Inc., Beverly, MA) that covers the *Eco*RI site in the multiple cloning site (Dale *et al.*, 1985). The size homogeneity of the linear molecules obtained was confirmed by EM measurements.

Coating of the ss DNA with RecA. The DNA recovered from four oocytes was mixed with 10 ng of linear ss M13mp19. RecA protein was added in a mass ratio of RecA:M13mp19 ss DNA of 80:1, in a total volume of 10 µl of 20 mM HEPES, pH 7.8, 100 mM KCl, 0.1 mM EDTA. After 15 min incubation at 37°C, 0.4 µl of 25% glutaraldehyde (Polysciences, Inc., Warrington, PA) was added to fix the complex. For EM, 5 µl of this reaction was mixed with 5–10 ng of uncoated ss linear and 10 ng of ds open circular M13mp19 DNA in a total of 80 µl of spreading solution.

Electron microscopy. The DNA was prepared for EM according to the formamide–cytochrome *c* monolayer technique (Davis *et al.*, 1971). The DNA was picked up on parlodion membranes, stained with uranyl acetate and shadowed with platinum–palladium (80:20). Preparations were observed with a JEOL JEM-100S electron microscope at 60 kV. Photographs were taken at a magnification of 10 000 on Kodak 4489 film. Molecular lengths were measured from prints (enlarged 33 or 66 times from the negatives) with a Numonics Graphics Calculator. Ds DNA, RecA-coated ss DNA and uncoated ss DNA were normalized separately to the appropriate size standards.

In order to estimate the number of crosslinks in the TMP-treated DNA, it was analyzed by EM under conditions of total denaturation. The DNA from 30 oocytes was denatured in the presence of 72% formamide

(redistilled, Bethesda Research Laboratories) and 0.5 M glyoxal (Fuka, Buchs, Switzerland) (Cech and Pardue, 1976; Revet and Benichou, 1981). Denatured DNA was prepared for EM (Revet and Benichou, 1981) and the minimal density of crosslinks was determined by the method of Revet and Benichou (1981). Using lightly crosslinked DNA, we have determined that no renaturation occurred during sample preparation; so the number of crosslinks should not be artificially overestimated.

Acknowledgements

We are grateful to the members of our laboratory for ideas and comments during this work. Dr Ed Maryon, Chris Lehman, Dave Segal and Shawn Christensen made helpful comments on the manuscript. We thank Dr Steve Kowalczykowski for a gift of RecA protein and Dr Jack Griffith for a gift of RecA protein and advice on its utilization. We thank Dr Oliver Richards for his advice on psoralen crosslinking techniques. The quality of the EM preparations was due in part to Dr Georges Picard's comments and Dr Edward King's help with EM equipment. We thank Jon Trautman for excellent technical assistance in the manipulation and injection of oocytes. Sanju Sharma assisted by making prints and performing some length measurements.

This work was made possible by grants from the US National Science Foundation (DMB-8718227 and MCB-9019139). G.P.-K. and R.J.D. were supported in part by a postdoctoral and predoctoral training grant from the National Cancer Institute (5T32 CA09602).

References

- Baur, M., Potrykus, I. and Dasakowski, J. (1990) *Mol. Cell. Biol.*, **10**, 492–500.
- Brouillette, S. and Chartrand, P. (1987) *Mol. Cell. Biol.*, **7**, 2248–2255.
- Carroll, D., Wright, S.H., Wolff, R.K., Grzesiuk, E. and Maryon, E.B. (1986) *Mol. Cell. Biol.*, **6**, 2053–2061.
- Cassuto, E. and Radding, C.M. (1971) *Nature*, **229**, 13–16.
- Cech, T.R. (1981) *Biochemistry*, **20**, 1431–1437.
- Cech, T.R. and Pardue, M.L. (1976) *Proc. Natl. Acad. Sci. USA*, **73**, 2644–2648.
- Chakrabarti, S., Joffe, S. and Seidman, M.M. (1985) *Mol. Cell. Biol.*, **5**, 2265–2271.
- Church, G.M. and Gilbert, W. (1984) *Proc. Natl. Acad. Sci. USA*, **81**, 1991–1995.
- Cortese, R., Harland, R. and Melton, D. (1980) *Proc. Natl. Acad. Sci. USA*, **77**, 4147–4151.
- Dale, R.M.K., McClure, B.A. and Houchins, J.P. (1985) *Plasmid*, **13**, 31–40.
- Davis, R.W., Simon, M. and Davidson, N. (1971) *Methods Enzymol.*, **21**, 413–428.
- Doherty, M.J., Morrison, P.T. and Kolodner, R.D. (1983) *J. Mol. Biol.*, **167**, 539–560.
- Dunn, K., Chrysogelos, S. and Griffith, J. (1982) *Cell*, **28**, 757–765.
- Feinberg, P.A. and Vogelstein, B. (1983) *Anal. Biochem.*, **132**, 6–13.
- Fishman-Lobell, J., Rudin, N. and Haber, J.E. (1992) *Mol. Cell. Biol.*, **12**, 1292–1303.
- Folger, K.M., Thomas, K. and Capecchi, M.R. (1985) *Mol. Cell. Biol.*, **5**, 59–69.
- Friedberg, E.C. (1985) *DNA Repair*. W.H. Freeman, New York.
- Goedecke, W., Vielmetter, W. and Pfeiffer, P. (1992) *Mol. Cell. Biol.*, **12**, 811–816.
- Gruss, C., Gutierrez, C., Burhans, W.C., DePamphilis, M.L., Koller, T. and Sogo, J.M. (1990) *EMBO J.*, **9**, 2911–2922.
- Grzesiuk, E. and Carroll, D. (1987) *Nucleic Acids Res.*, **15**, 971–985.
- Gurdon, J.B. and Wickens, M.P. (1983) *Methods Enzymol.*, **101**, 370–386.
- Hawley, R.S. (1988) In Kucherlapati, R. and Smith, G.R. (eds), *Genetic Recombination*. American Society for Microbiology, Washington DC, pp. 497–528.
- Hsieh, P., Camerini-Otero, C.S. and Camerini-Otero, R.D. (1990) *Genes Dev.*, **4**, 1951–1963.
- Jeong-Yu, S. and Carroll, D. (1992a) *Mol. Cell. Biol.*, **12**, 112–119.
- Jeong-Yu, S. and Carroll, D. (1992b) *Mol. Cell. Biol.*, **12**, in press.
- Kitamura, Y., Yoshikura, H. and Kobayashi, I. (1990) *Mol. Gen. Genet.*, **222**, 185–191.
- Lin, F.-L., Sperle, K. and Sternberg, N. (1984) *Mol. Cell. Biol.*, **4**, 1020–1034.
- Maryon, E. (1990) Ph.D. thesis, University of Utah, Salt Lake City, USA.
- Maryon, E. and Carroll, D. (1989) *Mol. Cell. Biol.*, **9**, 4862–4871.

- Maryon,E. and Carroll,D. (1991a) *Mol. Cell. Biol.*, **11**, 3268–3277.
Maryon,E. and Carroll,D. (1991b) *Mol. Cell. Biol.*, **11**, 3278–3287.
McEntee,K., Weinstock,G.M. and Lehman,I.R. (1979) *Proc. Natl. Acad. Sci. USA*, **76**, 2615–2619.
Ozenberger,B.A. and Roeder,G.S. (1991) *Mol. Cell. Biol.*, **11**, 1222–1231.
Pennington,S.L. and Wilson,J.H. (1991) *Proc. Natl. Acad. Sci. USA*, **88**, 9498–9502.
Plessis,A., Perrin,A., Haber,J.E. and Dujon,B. (1992) *Genetics*, **130**, 451–460.
Rao,B.J., Dutreix,M. and Radding,C.M. (1991) *Proc. Natl. Acad. Sci. USA*, **88**, 2984–2988.
Register,J.C. and Griffith,J. (1985) *J. Biol. Chem.*, **260**, 12308–12312.
Revet,B. and Benichou,D. (1981) *Virology*, **114**, 60–70.
Roth,D. and Wilson,J. (1988) In Kucherlapati,R. and Smith,G.R. (eds), *Genetic Recombination*. American Society for Microbiology, Washington DC, pp. 621–653.
Rubnitz,J. and Subramani,S. (1984) *Mol. Cell. Biol.*, **4**, 2253–2258.
Rudin,N. and Haber,J.E. (1988) *Mol. Cell. Biol.*, **8**, 3918–3928.
Seidman,M.M. (1987) *Mol. Cell. Biol.*, **7**, 3561–3565.
Seifert,H.S., Chen,E.Y., So,M. and Heffron,F. (1986) *Proc. Natl. Acad. Sci. USA*, **83**, 735–739.
Shibata,T., DasGupta,C., Cunningham,R.P. and Radding,C.M. (1979) *Proc. Natl. Acad. Sci. USA*, **76**, 1638–1642.
Smith,G.R. (1988) *Microbiol. Rev.*, **52**, 1–28.
Subramani,S. and Seaton,B.L. (1988) In Kucherlapati,R. and Smith,G.R. (eds), *Genetic Recombination*. American Society for Microbiology, Washington DC, pp. 549–574.
Sugawara,N. and Haber,J.E. (1992) *Mol. Cell. Biol.*, **12**, 563–575.
Sun,H., Treco,D. and Szostak,J.W. (1991) *Cell*, **64**, 1155–1161.
Symington,L., Morrison,P. and Kolodner,R. (1985) *J. Mol. Biol.*, **186**, 515–525.
Szostak,J.W., Orr-Weaver,T.L., Rothstein,R.L. and Stahl,F.W. (1983) *Cell*, **33**, 25–35.
Thomas,C.A. (1966) *Progr. Nucleic Acid Res. and Mol. Biol.*, **5**, 315–336.
Umlauf,S.W., Cox,M.M. and Inman,R.B. (1990) *J. Biol. Chem.*, **265**, 16898–16912.
Wallace,R.A. (1973) *J. Exp. Zool.*, **184**, 321–324.
West,S.C. (1990) *Bioessays*, **12**, 151–154.
White,C.I. and Haber,J.E. (1990) *EMBO J.*, **9**, 663–673.

Received on July 27, 1992; revised on September 25, 1992